DYNAMIC SCREENING VIA INTENSE LASER RADIATION AND ITS EFFECTS ON BULK AND SURFACE PLASMA DISPERSION RELATIONS

Steven Lanier

Thesis Prepared for the Degree of

MASTER OF SCIENCE

UNIVERSITY OF NORTH TEXAS

August 2017

APPROVED:

Yuri Rostovtsev, Major Professor
Duncan Weathers, Committee Leader
Paolo Grigolini, Committee Member
Michael Monticino, Interim Chair of the Department of Physics
David Holdeman, Dean of the College of Arts and Sciences
Victor Prybutok, Dean of the Toulouse Graduate School

Lanier, Steven. *Dynamic Screening via Intense Laser Radiation and Its Effects on Bulk and Surface Plasma Dispersion Relations*. Master of Science (Physics), August 2017, 32 pp., 17 figures, 11 numbered references.

Recent experimentation with excitation of surface plasmons on a gold film in the Kretschmann configuration have shown what appears to be a superconductive effect. Researchers claimed to see the existence of electron pairing during scattering as well as magnetic field repulsion while twisting the polarization of the laser. In an attempt to explain this, they pointed to a combination of electron-electron scattering in external fields as well as dynamic screening via intense laser radiation. This paper expands upon the latter, taking a look at the properties of a dynamic polarization function, its effects on bulk and surface plasmon dispersion relations, and its various consequences.

TABLE OF CONTENTS

LIST OF FIGURES

CHAPTER 1

INTRODUCTION

The interaction of electromagnetic waves and solids is an ever expanding topic. Ever since Maxwell's equations, the development of Solid-state physics has exploded. Among these topics is the existence of excitation's of oscillating charge densities throughout the system called plasmons. Alongside this bulk interaction, it was theorized that excitation of plasmons could exist on the surface of materials, along with accompanying electromagnetic waves bound to the surface, called surface plasmon polaritons (SPP), theorized by Rufus Ritchie in 1957 [9].

As an electromagnetic wave propagates through a material it causes oscillations in the electrons in the structure. The change in electron density then results in an opposing force fighting back against the perturbing force. This push and pull relation can be solved via the Maxwell equations, and their interactions fundamentally dictate the many electronic properties of the system, via the dielectric function. The dispersion relation of the electromagnetic wave in the medium follows from this interaction. Since electrons in metals are free, they tend to screen around local charges, screening them from outside sources. As far range interactions are decreased dramatically, how an electronic system feels an external perturbation changes , which changes how interactions play out. The dielectric function can then be solved more extensively, and shows numerous other properties than simple oscillations. Using this dynamic interaction to find the electronic response gives us the Lindhard function[3], an equation that relates the dielectric function to induced polarization via a screened response.

One of the many derivations of this function includes the idea that instead of free electrons, they are bound to an intense laser field with modulated wave-functions. This causes the lindhard function to change, cascading into everything it influences. This 'dynamic screening' function[11] is the core basis to this paper.

The inspiration for this paper arose when a group of Hungarian researchers saw what

they believed to be superconductive effects while experimenting with surface plasmons[7][8]. During experiments using Kretschmann configuration, they seemed to see electron pairing as well as magnetic field repulsion. Upon further examination, they observed an oscillatory change in the dispersion polaritons. They pointed to a paper by C. Zhang[11][6] as an explanation, claiming the dynamic polarization function as the basis to this oscillatory behavior.

This paper discusses basic theory including bulk plasmon and surface plasmon-polariton dispersion, as well as the mentioned dynamic screening function. It then expands upon their interactions and the consequences that arise.

CHAPTER 2

PLASMONICS

2.1. Maxwell's Equations

No paper involving electromagnetic waves can be written without first mentioning the father of all involved theory, the Maxwell equations. For electromagnetic waves in matter, we have

$$\nabla \cdot D = p_f \tag{2.1}$$

$$\nabla \cdot E = \frac{p}{\epsilon_0} \tag{2.2}$$

$$\nabla \cdot B = 0 \tag{2.3}$$

$$\nabla \times E = -\partial B/\partial t \tag{2.4}$$

$$\nabla \times H = J + \partial D/\partial t \tag{2.5}$$

$$D = \varepsilon_o \varepsilon E = \varepsilon_o E + P \tag{2.6}$$

$$B = \mu_0 H \tag{2.7}$$

Where ϵ_0 is the permitivity of free space, ϵ the permitivity of a specific medium, and μ_0 the magnetic permeability. From these, all following theory can be derived.

2.2. Dielectric Function

The dielectric function ϵ is among the most important variables in determining the electronic properties of the system. Working specifically in the long wavelength (small q) regime, the classical approximation for ϵ can be shown from the equation of motion of the free electron in the presence of a field, E[5].

$$m\frac{\partial^2 x}{\partial t^2} = -eE \tag{2.8}$$

Given that $E(t)$ and $x(t)$ depend on $e^{-i\omega t}$, it follows that

$$-\omega^2 mx = -eE, x = \frac{eE}{m\omega^2} \tag{2.9}$$

With $-ex$ being the dipole moment, and P being the polarization (dipole moment per unit volume, with n being electron concentration)

$$P = -nex = \frac{-ne^2 E}{m\omega^2} \tag{2.10}$$

now, with

$$D = \varepsilon\varepsilon_o E \tag{2.11}$$

$$\varepsilon = \frac{D}{\varepsilon_o E} = 1 + \frac{P}{\varepsilon_o E} \tag{2.12}$$

The classical dielectric function follows

$$\varepsilon(\omega) = 1 - \frac{ne^2}{\epsilon_0 m\omega^2} = 1 - \omega_p^2/\omega^2 \tag{2.13}$$

With the ω_p being the plasma frequency,

$$\omega_p = ne^2/m\varepsilon_0 \tag{2.14}$$

2.3. Plasmons

From the classical dielectric function, we can see $\varepsilon(\omega) = 0$ when the incoming frequency $\omega = \omega_p$. Large oscillations in the plasma occur via resonance when this happens. The quanta of energy for these oscillations of electron gas are called Plasmons, with energy $\hbar\omega_p$.

2.4. Dispersion Relation

Moving over to cgs from SI units (replacing $1/\epsilon_0$ with 4π), the basic wave equation in a non-magnetic medium is

$$\frac{\partial^2 D}{\partial t^2} = c^2 \nabla^2 E \tag{2.15}$$

which gives the dispersion relationship

$$\varepsilon(\omega)\omega^2 = c^2 K^2 \tag{2.16}$$

Which gives the plot (with ω_p set for gold)

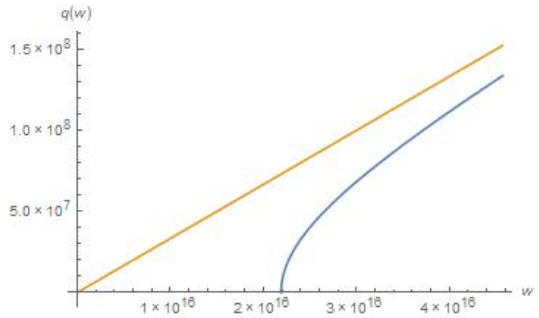

Wave vector $q(\omega)$ (written as k above) as a function of frequency ω. The yellow line is the vacuum relation $\omega * c$. The function bottoms out at the plasma frequency, with a forbidden range below it

FIGURE 2.1. Basic dispersion relation

2.5. Screening Effect

Due to the free nature of the electrons in the plasma, they tend to be influenced more by local charges, crowding around them and screening them from the outside. This drastically influences electromagnetic interactions inside the material, as the influence of local charges is highly diminished at long ranges.

Replacing the ω dependent dielectric function $\varepsilon(\omega)$ with its K dependent variant $\varepsilon(k)$ (derivation [5])

$$\varepsilon(k) = 1 - k_s^2/K^2 \tag{2.17}$$

where k_s is the Thomas-Fermi wave vector. The coulomb interaction $\frac{q}{r}$ is transformed to the classical screened potential

$$\frac{q}{r}e^{-k_s r} \tag{2.18}$$

showing the influence of a charge exponentially decays, almost removing long range interactions until at length $1/k_s$, the screening length.

2.6. Lindhard Function

A more complete method of calculating the dielectric function is to look at how the electronic system reacts to some arbitrary potential. This derivation in particular uses the random phase approximation, RPA, where the response to the system is dictated not by the induced potential but a total screened potential [3][10].

The Fourier transformed local (and assumed screened) potential can be represented as

$$\phi(r,t) = \iint (\phi(q,\omega)e^{i(q\cdot r-\omega t)}e^{(\delta t)} + \phi^* e^{-i(q\cdot r-\omega)t}e^{(\delta t)})dqd\omega \tag{2.19}$$

which we will use to perturb the system (δ is an infinitesimal to insure an adiabatic system). Under this, we can show the perturbed wave-function as a complete set with the unperturbed wave-function as the basis.

$$\psi_k(r,t) = \sum_{k'} a_{k'}(t)\psi^0_{k'}(r)e^{-i\epsilon_{k'}t/\hbar} \tag{2.20}$$

From the potential, we can see the allowed interaction states involve a_{k+q} and a_{k-q}. Expanding the wave-function, we have

$$\psi_k(r,t) = \psi^0_k(r)e^{-i\epsilon_k t/\hbar} + a_{k+q}(t)\psi^0_{k+q}(r)e^{-i\epsilon_{k+q}t/\hbar} + a_{k-q}(t)\psi^0_{k-q}(r)e^{-i\epsilon_{k-q}t/\hbar} \tag{2.21}$$

Solving for the coefficients under the time dependent perturbation theory, they become

$$a_{k+q}(t) = -i/\hbar \int_{-\infty}^{t} \langle\psi^0_{k+q}|H_1(t_1)|\psi^0_k\rangle e^{i(\epsilon_{k+q}-\epsilon_k)t_1/\hbar}dt_1 \tag{2.22}$$

$$a_{k-q}(t) = -i/\hbar \int_{-\infty}^{t} \langle\psi^0_{k-q}|H_1(t_1)|\psi^0_k\rangle e^{i(\epsilon_{k-q}-\epsilon_k)t_1/\hbar}dt_1 \tag{2.23}$$

Integrating over time (and space in the inner-product) gives

$$a_{k+q} = -\frac{\phi(q)e^{i(\epsilon_{k+q}-\epsilon_k-\hbar\omega)t/\hbar}e^{(\delta t)}}{\epsilon_{k+q}-\epsilon_k-\hbar\omega-(i\delta)} \tag{2.24}$$

$$a_{k-q} = -\frac{\phi^*(q)e^{i(\epsilon_{k-q}-\epsilon_k+\hbar\omega)t/\hbar}e^{(\delta t)}}{\epsilon_{k-q}-\epsilon_k+\hbar\omega-(i\delta)} \tag{2.25}$$

Expanding the full wave-function

$$\psi_k(r,t) = \psi^0_k(r)e^{-i\epsilon_k t/\hbar}[1 - \frac{\phi(q,\omega)e^{i(q\cdot r-\omega t)}e^{(\delta t)}}{(\epsilon_{k+q}-\epsilon_k-\hbar\omega-(i\delta))} - \frac{\phi^*(q,\omega)e^{-i(q\cdot r-\omega t)}e^{(\delta t)}}{(\epsilon_{k-q}-\epsilon_k+\hbar\omega-(i\delta))}] \tag{2.26}$$

Since (δt) is an infinitesimal, I'm going to leave it out of the calculations for now for convenience and throw it back in at the end. The induced density can be found from this.

$$p_k(r,t) = [|\psi_k(r,t)|^2 - |\psi_k^0(r)|^2] \tag{2.27}$$

With normalization giving the $\psi_k^0(r)$ component equal to 1 and keeping only terms linear to $\phi(q,\omega)$, ignoring ϕ^* for convenience

$$p_k(r,t) = -[\frac{\phi(q,\omega)e^{i(q\cdot r-\omega t)}}{\epsilon_{k+q} - \epsilon_k - \hbar\omega} + +\frac{\phi(q,\omega)e^{i(q\cdot r-\omega t)}}{\epsilon_{k-q} - \epsilon_k + \hbar\omega}] \tag{2.28}$$

Taking into account all states, the total density fluctuation can be represented as

$$p(r,t) = 2\sum_k p_k(r,t) f_k \tag{2.29}$$

where f_k is the fermi distribution function, and the factor of 2 due to spin states. With a change of variable from k to k+q in the term with ϵ_{k-w}, and using the Fourier relation ($p(r,t) \rightarrow p(q,\omega)$)

$$p(q,\omega) = 2\sum_k [\frac{f_{k+q} - f_k}{\epsilon_{k+q} - \epsilon_k - \hbar\omega}\phi(q,\omega)] \tag{2.30}$$

This gives the polarization function, Π_0, from $p(r,t) = \phi(q,w)\Pi(q,w)$, (along with adding the infinitesimal back in)

$$\Pi_0(q,w) = 2\sum_k [\frac{f_{k+q} - f_k}{\epsilon_{k+q} - \epsilon_k - \hbar\omega - i\delta} \tag{2.31}$$

The dielectric function in the RPA (random phase approximation), which uses the total screened potential response, finally becomes

$$\epsilon(q,w) = 1 - \frac{4\pi e^2}{q^2}\Pi_0(q,w) = 1 - \frac{4\pi e^2}{q^2}[2\sum_k \frac{f_{k+q} - f_k}{\epsilon_{k+q} - \epsilon_k - \hbar\omega - i\delta}] \tag{2.32}$$

Which is called the Lindhard Dielectric function ($\frac{4\pi e^2}{q^2}$ is $\phi(q)$).

Using different approximations, familiar results can be achieved. In the long wavelength limit ($q \Rightarrow 0$) and the static limit ($\omega \Rightarrow 0$), and assuming the potential is slowly varying with respect to the electron wavelength, the Lindhard function reduces roughly to

$$\epsilon(w) = 1 - \omega_p^2/\omega^2 \tag{2.33}$$

and

$$\epsilon(q) = 1 + k_s^2/q^2 \tag{2.34}$$

where k_s is the Thomas-Fermi wave vector.

From this we can plot the normal dielectric and corresponding dispersion relation, $q(w) = \omega/c\sqrt{\epsilon(w)}$

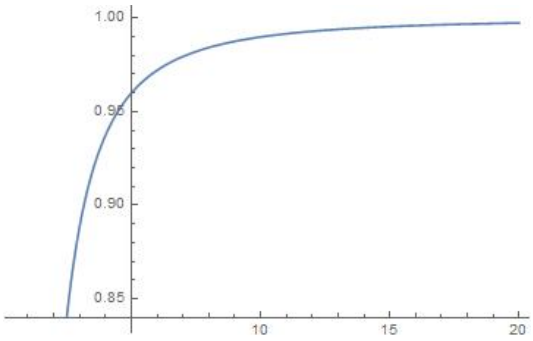

Dielectric ϵ as a function of ω, with arbitrary unit values

FIGURE 2.2. Dielectric function

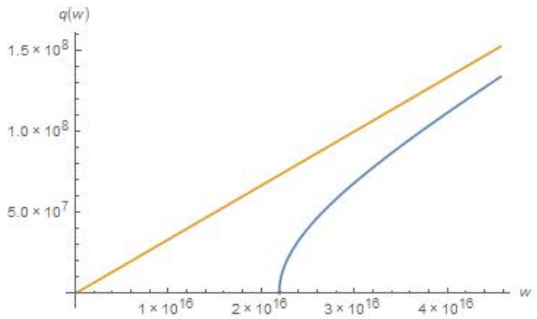

Wave vector q as a function of ω, with ω_p set for gold

FIGURE 2.3. Basic dispersion relation

2.6.1. Low Temperature Limit

Taking the polarization function $\Pi(q, w)$, and applying the limit as temperature T $\rightarrow 0$, we can write the function as[3]

$$\sum_{k<k_f, k+q>k_f} [\frac{1}{\hbar\omega - \epsilon_{k+q} + \epsilon_k} - \frac{1}{\hbar\omega - \epsilon_k + \epsilon_{k+q}}] \tag{2.35}$$

Graphing this gives

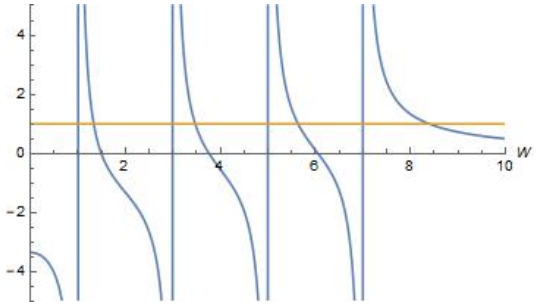

Polarization function Π dependence on ω, with arbitrary unit values

FIGURE 2.4. Polarization function

The poles in the graph correlate to electron-hole pair formations, with an upper value ω_{max} above which has no more pairs. The right end tail intersection with the horizontal line at 1 (with $\phi(q)$ normalized to 1) corresponds to the plasma frequency ω_p, which involves large scale plasma oscillations instead of individual particle excitation.

CHAPTER 3

DYNAMIC SCREENING

3.1. Dynamic Screening Function

In the previous section the basic Lindhard function was derived using the perturbation of free electrons by the total screened interaction. This section involves the same idea, except instead of a free electron we use a wave-function modified by an external field, shown here [11].

As mentioned, we will modify the basic free electron wave-function

$$\psi(r,t) = \exp(ik \cdot r) \exp\left(-it\epsilon_k\right); \tag{3.1}$$

$$\epsilon_k = \frac{k^2}{2m^*} \tag{3.2}$$

with an external field, with the potential in the form

$$A = \frac{E\sin(\omega t)}{\omega} e_x \tag{3.3}$$

Where the time dependent Schrödinger equation in an external field is transformed by

$$U = \exp\left(2\gamma_1 itw\right) \exp\left[\gamma_0 ik_x(1-\cos(tw)\right) \exp\left(\gamma_1 i\sin(2tw)\right) \tag{3.4}$$

$$\gamma_0 = (eE)/m^*\omega^2, \gamma_1 = (eE)^2/(8m^*\omega^3) \tag{3.5}$$

a unitary operator, where

$$U[i\frac{\partial\psi(r,t)}{\partial t} - \frac{p^2}{2m*}] = i\frac{\partial}{\partial t} - \frac{(p-Ae)^2\psi(r,t)}{2m^*} \tag{3.6}$$

$$i\frac{\partial\psi(r,t)}{\partial t} = H\psi(r,t) = \frac{(p-Ae)^2\psi(r,t)}{2m^*} \tag{3.7}$$

The wave-function is

$$\psi_k^0(r,t) = Uexp(-i\epsilon_k t)exp(ik\cdot r) \tag{3.8}$$

Make $F(t) = 2\gamma_1\omega t + \gamma_1 sin(2\omega t)$, then

$$\psi_k^0(r,t) = e^{iF(t)}e^{i\gamma_0 k_x(1-cos(\omega t)}e^{ik\cdot r}e^{-i\epsilon_k t} \tag{3.9}$$

$$\langle\psi_k^0(r,t)|\psi_k^0(r,t)\rangle = \delta_{k,k'} \tag{3.10}$$

From this, the wave-function is still normalized, so no charge fluctuation

$$p_k^0 = e|\psi_k^0(r,t)|^2 = e \tag{3.11}$$

Using this wave-function as the basis for the complete set, we can follow the same process as before.

$$\psi(r,t) = \sum_k a_k(t)e^{iF(t)}e^{i\gamma_0 k_x(1-cos(\omega t))}e^{ik\cdot r}e^{i\epsilon_k t} \tag{3.12}$$

with the Fourier transformed local potential given again as

$$\phi(r,t) = \int dq' \int d\Omega e^{iq'\cdot r}e^{-i\Omega t}\phi(q',\Omega) + \int dq' \int d\Omega e^{-iq'\cdot r}e^{i\Omega t}\phi(q',\Omega) \tag{3.13}$$

Using this as the perturbing potential, the coefficients are solved for

$$i\frac{\partial\psi}{\partial t} = (H - e\phi)\psi \tag{3.14}$$

$$a'_k(t) = -ie\int_{-\infty}^{\infty} dt e^{i\gamma_0(k_x-k'_x)[1-cos(wt)]}e^{i(\epsilon_{k'}-\epsilon_k)t} \times \int dr e^{-ik'\cdot r}\phi(r,t)e^{ik\cdot r} \tag{3.15}$$

Using the Generating Bessel function

$$e^{iacosx} = \sum_m i^m J_m(a)e^{imx} \tag{3.16}$$

and the Fourier expansion for the local potential, you get

$$a_{k+q} = -ee^{-i\gamma_0 q_x}\sum_{m,\Omega} i^m J_m(q_x\gamma_0)\phi(q,\Omega) \times \frac{e^{i(\epsilon_{k+q}-\epsilon_k-\Omega-m\omega)t}}{\epsilon_{k+q}-\epsilon_k-\Omega-m\omega-i\delta} \tag{3.17}$$

$$a_{k-q} = -ee^{-i\gamma_0 q_x}\sum_{m,\Omega} i^m J_m(q_x\gamma_0)\phi(q,\Omega) \times \frac{e^{i(\epsilon_{k-q}-\epsilon_k+\Omega+m\omega)t}}{\epsilon_{k-q}-\epsilon_k+\Omega+m\omega-i\delta} \tag{3.18}$$

with the infinitesimal $i\delta$ back in as before. Plugging these into

$$\psi_k(r,t) = \psi^0_k(r,t) + \sum_q a_{k\pm q}(t)\psi^0_{k\pm q}(r,t) \tag{3.19}$$

the induced charge density is

$$p_k(r,t) = e[|\psi_k(r,t)|^2 - |\psi^0_k(r)|^2] \tag{3.20}$$

$$\begin{aligned} p_k(r,t) = -e^2\sum_{q,\Omega}\sum_m i^m\phi(q,\omega)J_m(q_x\gamma_0)\times \\ [\frac{e^{-i\gamma_0 q_x cos(wt)}e^{-i(\Omega+mw)t}}{\epsilon_{k+q}-\epsilon_k-\Omega-m\omega-i\delta}e^{iq\cdot r} \\ +\frac{(-1)^m e^{i\gamma_0 q_x cos(wt)}e^{i(\Omega+mw)t}}{\epsilon_{k-q}-\epsilon_k+\Omega+m\omega+i\delta}e^{iq\cdot r}] \end{aligned} \tag{3.21}$$

This is similar to the derived original Lindhard density function,

$$p_k(r,t) = -[\frac{\phi(q,\omega)e^{i(q\cdot r-\omega t)}}{\epsilon_{k+q}-\epsilon_k-\hbar\omega-i\delta} + +\frac{\phi(q,\omega)e^{i(q\cdot r-\omega t)}}{\epsilon_{k-q}-\epsilon_k+\hbar\omega-i\delta}] \tag{3.22}$$

Using the generating Bessel function again on $e^{-i\gamma_0 q_x cos(wt)}$

$$e^{iacosx} = \sum_m i^m J_m(a)e^{imx} \tag{3.23}$$

the dielectric function can be found, with a slight difference

$$\epsilon(q,w) = 1 - \frac{4\pi e^2}{q^2}\Pi(q,w) = 1 - \frac{4\pi e^2}{q^2}\sum_m J_m^2(q_x\gamma_0)[\sum_k \frac{f_{k+q}-f_k}{\epsilon_{k+q}-\epsilon_k-\Omega-m\omega-i\delta}] \tag{3.24}$$

where

(3.25)

$$\Pi(q,\Omega+m\omega) = \sum_m J_m^2(q_x\gamma_0)[\sum_k \frac{f_{k+q}-f_k}{\epsilon_{k+q}-\epsilon_k-\Omega-m\omega-i\delta}] = \sum_m J_m^2(q_x\gamma_0)\Pi_0(q,\Omega+m\omega)$$

In all, the dynamic function has a very similar form as the original lindhard function, with two notable exceptions: A squared Bessel function, dependent on the wave vector, frequency, and intensity of the laser, and an additional frequency term on the bottom with integer m. Both summed for m over infinity.

3.2. Analyzing the Excited Lindhard Function

If we apply the same $T \to 0$ limit as before, we can plot the polarization as a function of ω and static laser intensity (in the form of amplitude E) with $a = eE/cm^*$, turning $J^2(q_x\gamma_0) \to J^2(q_x a/\omega^2)$. Here I take arbitrary values of q, a, and ω, just to view the behavior function, with all other values set to unity(1).

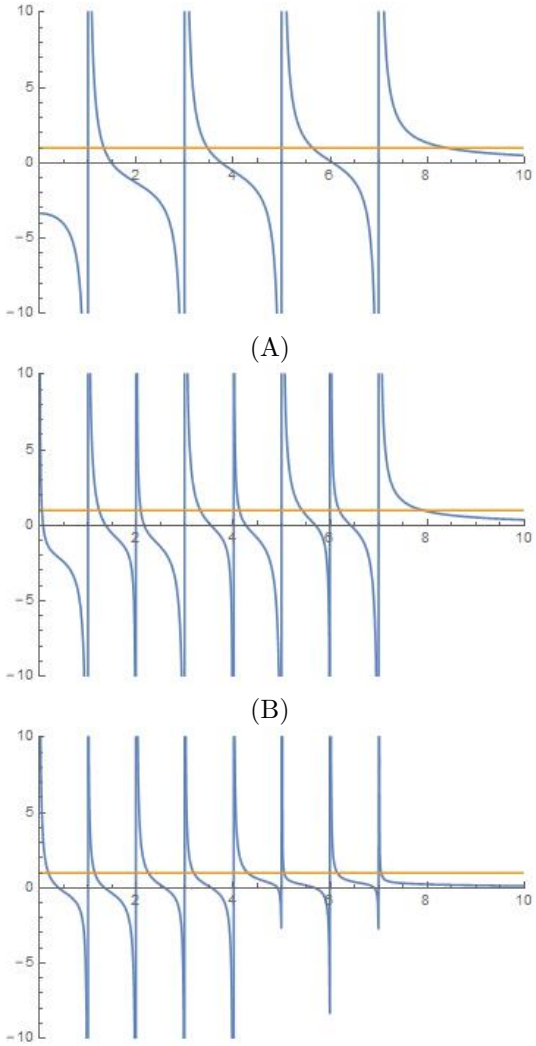

(A)

(B)

(C)

Π as a function of ω, with increasing field intensities going from a to c

FIGURE 3.1. Excited polarization function

It is evident that turning on the laser and increasing the intensity adds a multitude of poles to the function. This is a result of the multi-photon processes influencing the available number of excitation states. As well, with increasing intensity comes a suppression of the plasma frequency.

Spreading out the function to include more states

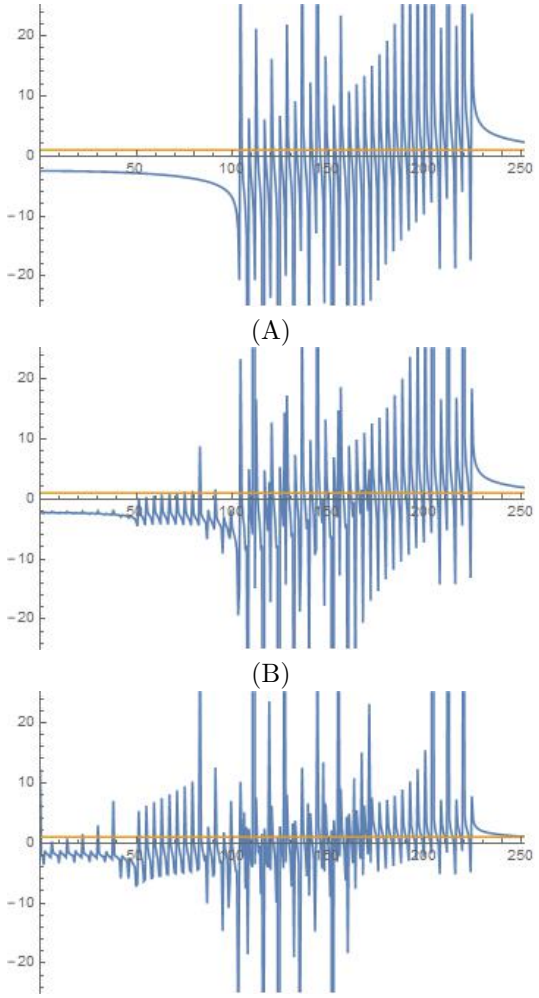

Π as a function of ω, with increasing field intensity for each graph

FIGURE 3.2. Excited polarization function, expanded

Again as before, there is a large increase in available excitation states, including many in the previously empty zone below the minimum required frequency for excitation.

Looking at the far end (again with arbitrary absolute values), the lowering of the plasma frequency becomes more clear.

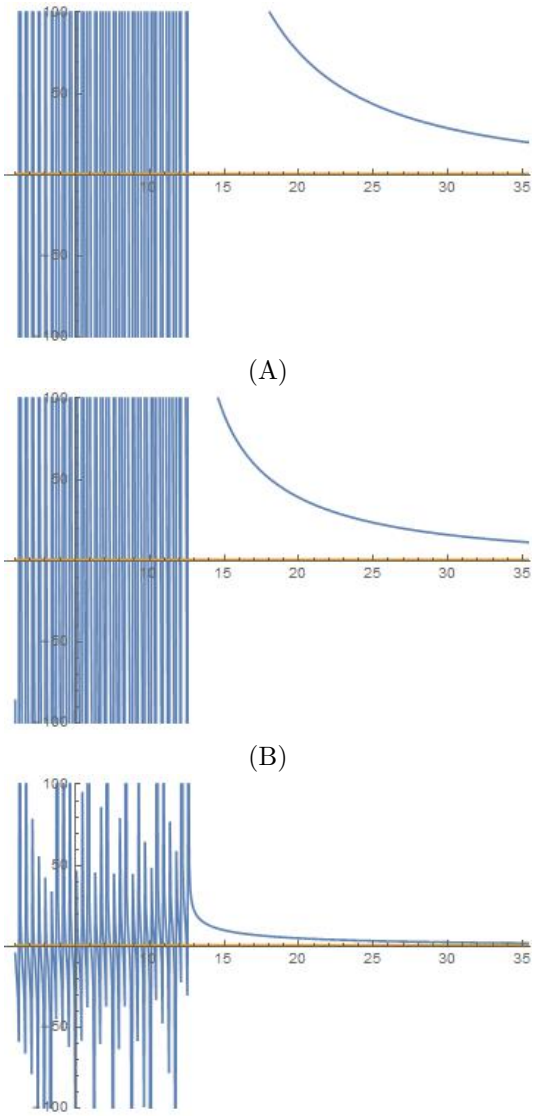

(A)

(B)

(C)

Π as a function of ω with continually increased field intensity for each graph

FIGURE 3.3. Tail of excited polarization function

Since the primary application of this theory will be on surface plasmons, another interesting regime is to take $\Omega = \omega$ considering the excited polaritons will share the same frequency as the incident laser. Graphing, the function take on an oscillatory behavior on the far tail in with increasing intensity

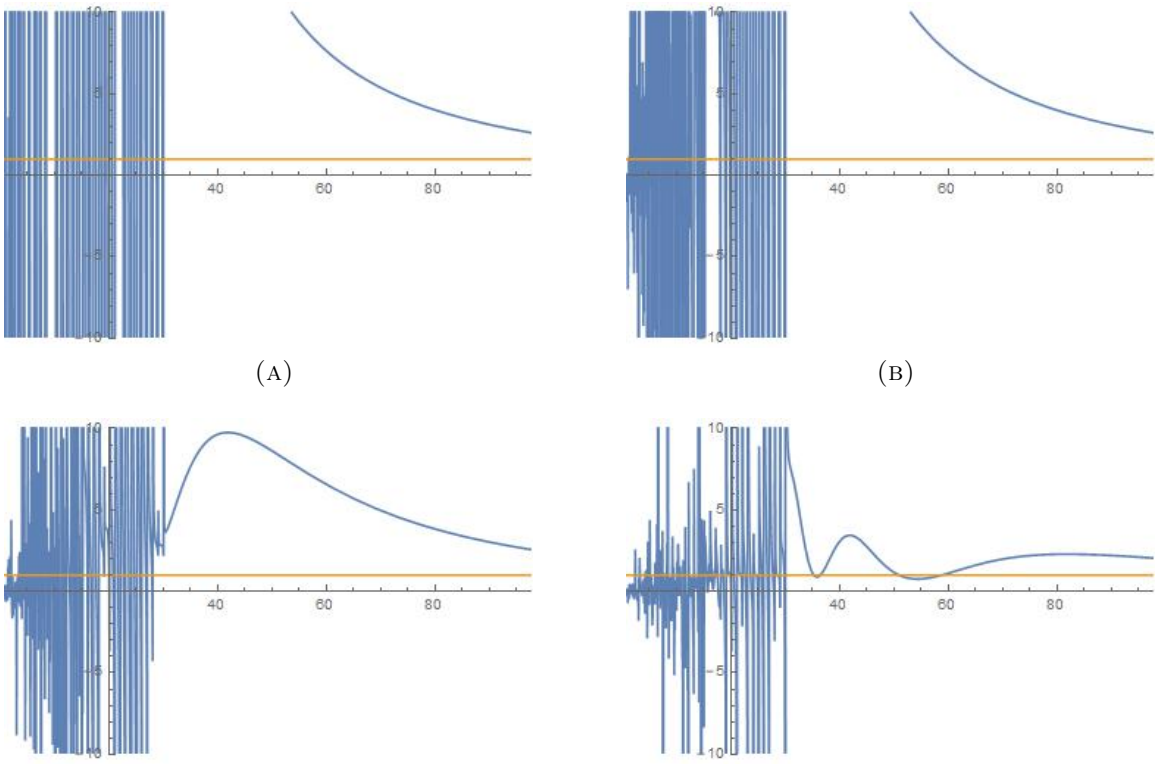

(A) (B)

(C) (D)

Π as a function of ω, with continually increased field intensity from A to D

FIGURE 3.4. Tail of excited polarization function, $\Omega = \omega$

Not only is there a suppression of plasma frequency, but more modes involving ω_p. The higher the intensity, the more available plasma frequency modes are present. Essentially, it is opening up holes in the spectrum for electromagnetically induced transparency.

3.2.1. Long Wavelength Limit

Applying the same limits to the dynamic polarization function as before to the normal Lindhard function, taking $q \to 0$ and $T \to 0$, as well working with frequencies $\Omega = \omega$ [6]

The polarization function

$$\Pi(q, \omega) = \sum_m J_m^2(q_x \gamma_0) \Pi_0(q, \omega + mw) \tag{3.26}$$

can be reduced to

$$\phi(q)\Pi(\omega) = \frac{\omega_p^2}{\omega^2} \sum_m \frac{J_m^2(q_x\gamma_0)}{(1+m)^2} \tag{3.27}$$

Taking the function g(w) where $w = q_x\gamma_0$ (where $\gamma_0 = (eE)/m^*\omega^2$)

$$g(w) = \sum_m \frac{J_m^2(w)}{(1+m)^2} \tag{3.28}$$

and plotting with unit values set to unity again to show the behaviour dependence on intensity (noting w =/= ω)

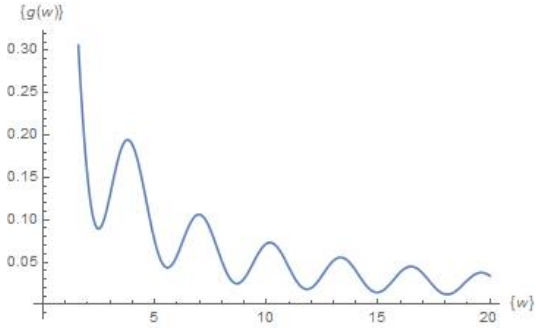

Oscillating function g(w) dependence on intensity (via w = $q_x\gamma_0$)

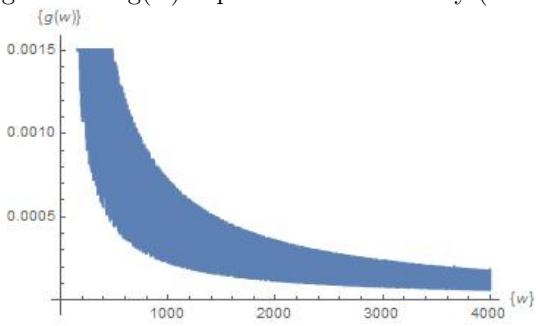

Increased intensity range

FIGURE 3.5. Oscillating dependence on field intensity

The function shows a clear oscillatory behavior, with a decreasing amplitude for increasing intensity (and obviously reversed for its dependence on ω).

Taking this approximated dynamic polarization function, assuming low q where qc/ω is roughly linear (so $qc/\omega \approx 1$, then w $\rightarrow eE/cm * \omega$) we can plot the classical dispersion relation

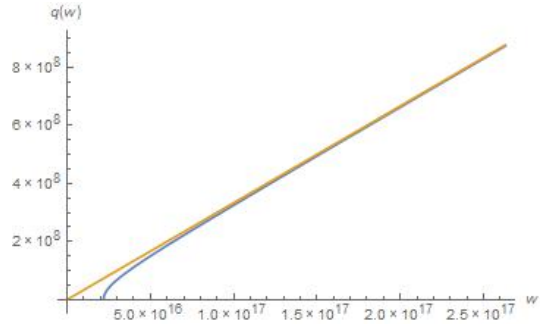

$q(\omega) = w/c * \sqrt{\epsilon(\omega)}$, with low arbitrary intensity

FIGURE 3.6. Dispersion relation

And you get, at low intensity, the same dispersion relation as normally.

Looking at the functions at high intensity however shows a different result.

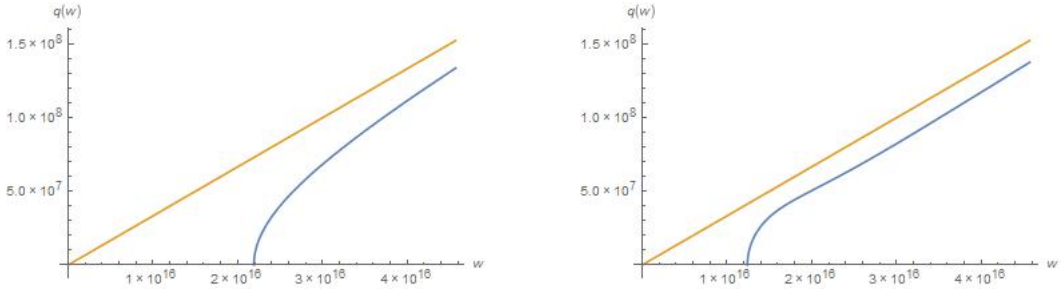

(A) (B)

Dispersion relation, showing wave vector q as a function of ω with each graph having increased laser field intensity

FIGURE 3.7. Modified dispersion relation

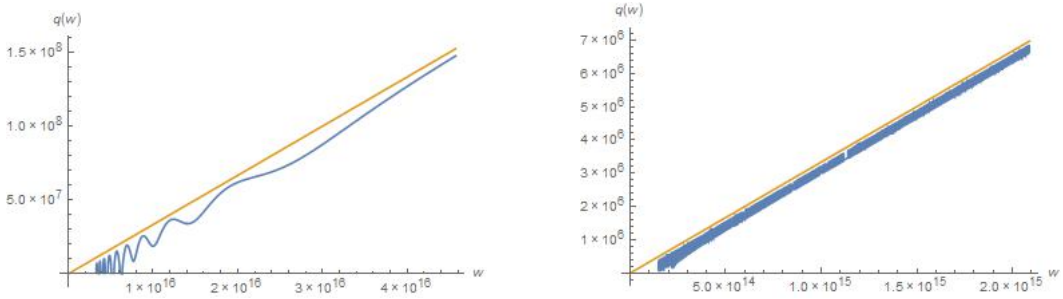

(A) (B)

Dispersion relation, showing wave vector q as a function of ω with each graph having increased laser field intensity

FIGURE 3.8. Modified dispersion

Zooming in on the function, we can see 'holes' opening up in the spectrum.

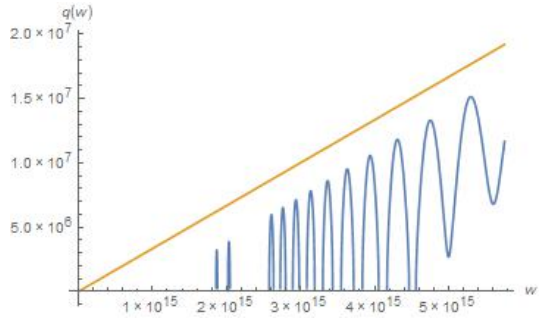

(A)

FIGURE 3.9. Plasma modes increased

Evidently the function shows with increased intensity comes a decreased plasma frequency and an opening of multiple plasma frequencies, with allowed and disallowed regions in between. This matches up with the interpretation from the results of the un-approximated dynamic polarization function. One source of inaccuracy though, is this does not follow the q linear with ω rule set before. However, the behavior that causes it, the Bessel function,is still in the approximation,. So while the exact numbers may not match up the overall behavior should still exist.

CHAPTER 4

SURFACE PLASMON POLARITONS

Surface plasmons, a phenomenon predicted back in 1957 by Rufus Ritchie[9], are electron density oscillations that occur on the surface, with different modes then related bulk plasmons. Existing with the surface plasmon is the propagation of an electromagnetic wave bound to the surface (and the underlying plasma oscillations) called a surface plasmon polariton.

To derive, we look at a classical model of a semi infinite system,treating μ as 1 and assuming the absence of external sources. Giving two medium a plane at $z = 0$, with $z < 0$ as ϵ_1, and $z > 0$ as ϵ_2 (more thoroughly found [9])

$$\nabla \times H_i = \epsilon_i \frac{1}{c} \frac{\partial}{\partial t} E_i \tag{4.1}$$

$$\nabla \times E_i = -\frac{1}{c} \frac{\partial}{\partial t} H_i \tag{4.2}$$

$$\nabla \cdot (\epsilon_i E_i) = 0 \tag{4.3}$$

$$\nabla \cdot H_i = 0 \tag{4.4}$$

where i determines the material at the boundary. The boundary conditions (given in Jackson's Classical Electrodynamics)

$$D_{1,z} = D_{2,z} \tag{4.5}$$

$$B_{1,z} = B_{2,z} \tag{4.6}$$

$$E_{1,x/y} = E_{2,x/y} \tag{4.7}$$

$$H_{1,x/y} = H_{2,x/y} \tag{4.8}$$

It can be shown that S-polarization for incoming light cannot form propagating waves on the surface and as such, it must be P-polarized with magnetic field H parallel to the surface[[9][4]]. Choosing the X direction as the propagation vector on the surface, there are components of the electric field in the direction of propagation as well as an exponentially decaying component in the Z direction, normal to the surface[1].

$$E_i = (E_{i_x}, 0, E_{i_z}) = e^{-\kappa_i |z|} e^{i(q_i x - \omega t)} \tag{4.9}$$

$$H_i = (0, H_{i_y}, 0) e^{-\kappa_i |z|} e^{i(q_i x - \omega t)} \tag{4.10}$$

Plugging these into the boundary conditions and Maxwell's equations above gives

$$i\kappa_1 H_{1_y} = (\omega/c)\epsilon_1 E_{1_x} \tag{4.11}$$

$$i\kappa_2 H_{2_y} = (-\omega/c)\epsilon_2 E_{2_x} \tag{4.12}$$

with the z-component being

$$\kappa_i = \sqrt{q_i^2 - \epsilon_i \omega^2/c^2} \tag{4.13}$$

Knowing that the boundary conditions define continuity for the parallel components of E and B,

$$\frac{\kappa_1}{\epsilon_1} H_{1_y} + \frac{\kappa_2}{\epsilon_2} H_{2_y} = 0 \tag{4.14}$$

and

$$H_{1_y} - H_{2_y} = 0 \tag{4.15}$$

Which gives the surface plasmon condition [9]

$$\frac{\epsilon_1}{\kappa_1} + \frac{\epsilon_2}{\kappa_2} = 0 \tag{4.16}$$

The boundary conditions further imply $q_1 = q_2 = q$. Solving for q in the equation above gives us

$$q(\omega) = \frac{w}{c}\sqrt{\frac{\epsilon_1\epsilon_2}{\epsilon_1 + \epsilon_2}} \tag{4.17}$$

In the classical long-wavelength model with $\epsilon_1 = 1 - \omega_p^2/\omega^2$ and $\epsilon_2 = 1$ for a vacuum, the equation becomes

$$q(\omega) = \frac{w}{c}\sqrt{\frac{\omega^2 - \omega_p^2}{2\omega^2 - \omega_p^2}} \tag{4.18}$$

Solving for ω gives

$$\omega^2(q) = \omega_p^2/2 + c^2q^2 \pm \sqrt{w_p^2/4 + c^4q^4} \tag{4.19}$$

Plotting $q(\omega)$ then gives

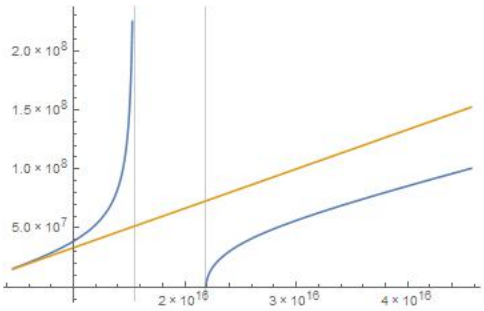

Left blue line is SPP dispersion, right blue line is photon disperion through material. Left grey line is $\omega_p/\sqrt{2}$, right grey line is ω_p for gold

FIGURE 4.1. Surface plasmon dispersion relation

This is the dispersion function (reversed, $q(\omega)$ instead of $\omega(q)$) for surface plasmon polaritons. There is classically a gap in between, where the dielectric function leads to imaginary results, causing the incoming radiation to be reflected with no surface propagation. As well, the dispersion line for the polaritons lies above the $q = w/c$ line leading to free

radiation being unable to excite surface plasmons. In order to get around this, setups such as gratings on the surface, or refraction via prisms (Kretschmann configuration) may be used.

CHAPTER 5

SURFACE PLASMON POLARITONS AND DYNAMIC SCREENING

Now that the basics of SPP dispersion have been laid out, we can move into the dynamically screened dispersion relation. Taking a look at the dynamic polarization function

$$\Pi(q, \Omega + m\omega) = \sum_m J_m^2(q_x\gamma_0)\Pi_0(q, \Omega + m\omega) \tag{5.1}$$

we apply the same limits as before. Taking $q \to 0$ and $T \to 0$, and working with frequencies $\Omega = \omega$ and with ω_p set for gold, we use the function

$$\phi(q)\Pi(\omega) = \frac{\omega_p^2}{\omega^2} \sum_m \frac{J_m^2(q_x\gamma_0)}{(1+m)^2} \tag{5.2}$$

and plug the calculated ϵ into $q(\omega) = \frac{w}{c}\sqrt{\frac{\epsilon_1\epsilon_2}{\epsilon_1+\epsilon_2}}$, treating ϵ_2 as 1 and $q_x\gamma_0$ as $eE/cm * \omega$ (where I took $q_x c/\omega \to 1$, mimicking [6])

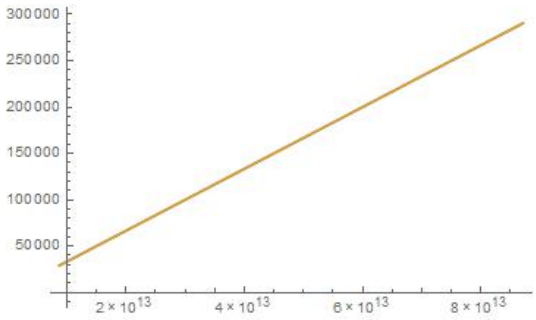

$q(\omega)$as a function of frequency, with arbitrarily low intensity

FIGURE 5.1. SPP low q dispersion

Looking at low q values, this mimics the classical dispersion relation and is linear to the vacuum dispersion $qc/\omega = 1$. Increasing intensity turns on an oscillatory behavior as well as a slowly increasing q, varying off of the vacuum line

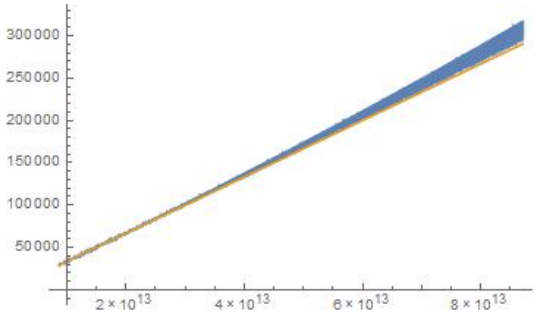

$q(\omega)$ with arbitrarily increased intensity

FIGURE 5.2. SPP low q excited dispersion

Breaking the approximation setting set earlier (a linear q/w relation) and looking towards the classic split between surface plasmon polariton dispersion and photon dispersion, a new shape appears

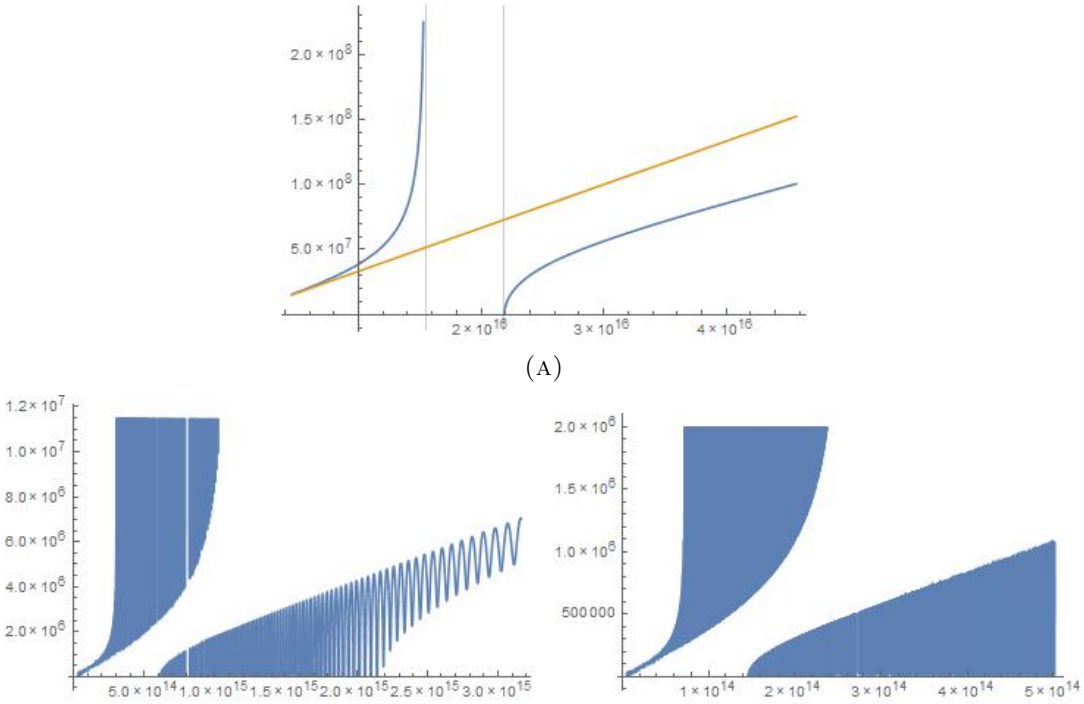

(A)

(B) (C)

Surface plasmon polariton dispersion relation varying from no laser field (A) to arbitrarily high laser field (C)

FIGURE 5.3. SPP excited disperison

When introducing high intensity into the play, the dispersion relation takes on a whole new shape. A broad thickness appears due to high frequency oscillations in the polarization

function. This mimics the bulk dispersion pattern, showing multiple new plasma frequencies. As well, the original gap that existed between $\omega_p/\sqrt{2}$ and ω has now been closed. There is an overlap in allowed frequencies, giving rise to the possibility of surface plasmon polariton and bulk photon propagation at the same time (although in a very dynamic fashion, with each allowed state being out of phase). The true shape in this region, especially for the line on the left given its explosion of q, will not look exactly as shown. But the behavior that causes it, $\sum_m \frac{J_m^2(q_x\gamma_0)}{(1+m)^2}$, exists regardless of which approximation you use. In fact, the value inside of the bessel function will increase in the presence of large q, possibly causing a more extreme version of what we see here. Further investigation in this region warrants solving the system in a self-consistent manner.

CHAPTER 6

SPECIAL TOPICS

6.1. Experimental Verification

All of this was fundamentally inspired by experimental data. The original derivation of the dynamic screening function claimed an oscillatory nature depending on the wavelength of incoming radiation and a decreased plasma frequency for an increased laser intensity. Recent papers from Hungary [6] claim this dynamic screening model also caused the oscillatory behavior and general increased value of the wave-vector dependence in their absorption spectrum. All of these effects have been shown to exist in various ways in this expanded analysis, with the caveat of some inappropriate looks outside approximation domains. As mentioned before, the cause of the behavior, the Bessel function, still exists in the un-approximated solutions. Experimental verification gives validity to the interpreted consequences, and inspire a more self-consistent approach to be solved.

6.2. Superconductive Observation

One cause for an increased look into this particular theory behind femtosecond laser interactions with surface plasmons is the claimed evidence of superconductivity in recent experiments by the same group [[7] [8]]. They claim that this is caused by the intense electromagnetic waves on the surface inducing a negative potential, as shown in a paper deriving electron-electron scattering in external fields [2]. By finding a theory to appropriately describe the electronic system present, we can move forward and attempt to find more precisely the nature of this observation, whether its a multitude of matter interactions or instead solely due to the electron scattering in intense fields. Regardless this will be a large inspiration moving forward.

6.3. Ideas for Future Experiments

Following the current experiment, a similar one will be performed by adding gratings on the surface. Other potential scenarios range from thinning out the gold further, to going

the other way and looking at the possibility of surface excitation on bulk materials, if it is indeed possible for SPP and normal photon dispersion as predicted above. While performing additional experimentation, it will be interesting to see how well this theory holds up and whether the phenomena predicted in the poor approximation zones really exist or if some approximated-out effect prevents them in real dynamically evolving environments.

CHAPTER 7

CONCLUSION

This paper has shown a variety of effects that arise in the case of laser-stimulated electron systems. The dynamic screening function affects the core behaviour inside of the metal, including plasmon to surface plasmon dispersion relations. We can see the experimentally found plasma frequency suppression and oscillatory behavior of the allowed wave vectors match up with the theoretical models proposed. In addition, new electron-hole excitation via multi-photon processes can be found, as well as new modes of plasma excitation and a potential overlap in allowed frequencies for bulk and surface plasmon oscillations. These consequences will ultimately shape future development.

REFERENCES

[1] Oliver Benson, *Plasmonics*, www.physik.hu-berlin.de/de/nano/lehre/ (2009), Gastvorlesung Plasmonics.

[2] J Bergou, S Varro, and M V Fedorov, *e-e scattering in the presence of an external field*, J Bergou et al J. Phys. A: Math. Gen. 14 2305 (1981).

[3] Peter Hirschfeld, *Electron-electron interactions*, http://www.phys.ufl.edu/ pjh/teaching/phz7427/7427notes/ch2.pdf (2013).

[4] John David Jackson, *Classical electrodynamics third edition 3rd edition*, Wiley, 1998.

[5] Charles Kittel, *Solid state physics 8th edition*, Wiley, 2005.

[6] N. Kroó, P. Rácz, and I. Tüttő, *Plasmonic dynamic screening in a gold film by intense femtosecond laser light*, EPL, 115 27010 ((2016)).

[7] N. Kroó, P. Rácz, and S. Varró, *Surface plasmon assisted electron pair formation in strong electromagnetic field*, EPL, 105 67003 (2014).

[8] N. Kroó, P. Rácz, and S. Varró., *Surface-plasmon assisted magnetic anomalies on room temperature gold films in high-intensity laser fields*, EPL, 110 67009 (2015).

[9] J M Pitarke, V M Silkin, E V Chulkov, and P M Echenique, *Theory of surface plasmons and surface-plasmon polaritons*, Rep. Prog. Phys. 70 (2007) 1–87.

[10] Jenö Sólyom, *Fundamentals of the physics of solids*, vol. 3, 2010.

[11] C. Zhang, *Dynamic screening and collective excitation of an electron gas under intense terahertz radiation*, 65, 153107 (2002).